Clock Products Working Group

K. Senior

U.S. Naval Research Laboratory
4555 Overlook Ave SW; Washington DC 20375
`ken.senior@nrl.navy.mil`; Phone: $+1\,202\,767\,2043$

In 2011 the IGS Clock Products Working Group (CPWG) migrated the IGS Rapid and Final clock products to new reference timescales based on a new version 2.0 algorithm developed at the U.S. Naval Research Lab (NRL). The new algorithm was implemented primarily to improve upon the longer term stability of the legacy v1.0 timescale. The improvements include changes to clock modeling, the UTC alignment (steering), as well as to changes to the clock weighting approach used. Additional states were also added to the Kalman filter to model up to two fixed period harmonics in order to better compensate contributions from the GPS satellite clocks. The algorithm is fully automated requiring no regular user intervention. A brief description of the algorithm improvements is given below along with its current performance status.

1 Basic Model for all Clocks

The basic clock model used for each clock in the new version 2.0 IGS timescale (both ground and GPS satellite clocks) includes the clock's time (or phase), its first derivative
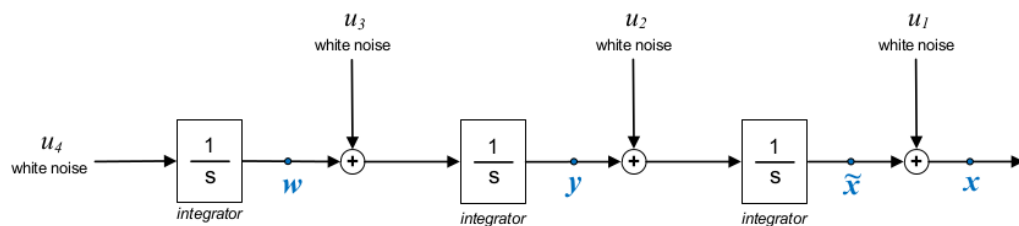

Figure 1: The basic clock model used in the IGS v2.0 timescale includes the clock's phase x, frequency y, and drift w, each driven by integrated white noises (random walks) as well as an additional phase state $\tilde{x}$, necessary to model also a pure white phase noise. Up to two pure harmonics may also be included. Each of the phase, frequency, and drift states are modelled stochastically by an independent random walk, random walk phase (RWPH), random walk frequency (RWFR), and random walk drift (RWDR).

(frequency), and its second derivative (drift), each modeled stochastically with an independent random walk as shown in Figure 1. An additional phase state $\tilde{x}$ is included to model a pure white phase noise and to couple to optionally specified pure fixed period harmonics as described below.

The perfect integrator model of Figure 1 (or subcomponents of it) has been used to model well the behavior of most clocks dating back to the 80 s (Jones and Tryon, 1983). Although the legacy version of the IGS timescale employed only a two state model of a clock's behavior the new version has employed the new full version.

2 Additional Pure Harmonic States

It has been well investigated that significant harmonics are present throughout the GPS constellation clocks nominally at periods of 12–h, 6–h, 4–h and 3–h with amplitudes up to 2 ns (c.f., Senior et al., 2008; Montenbruck et al., 2011). Figure 2 shows the amplitude spectra of the GPS constellation clocks where all spectra were calculated individually for each clock and then averaged over the constellation in the Fourier domain. As the figure shows the pervasiveness and prominence of particularly the 12–h and 6–h harmonics in most GPS satellite clocks dictates the need to compensate or model these variations explicitly in the timescale filter. For this reason four additional states have been included in the v2.0 IGS timescale filter to compensate up to two fixed period harmonics which can be specified per clock. Two states are required for each harmonic, one in–phase and one quadrature, and are coupled only to a single phase state as shown in Figure 1 above.
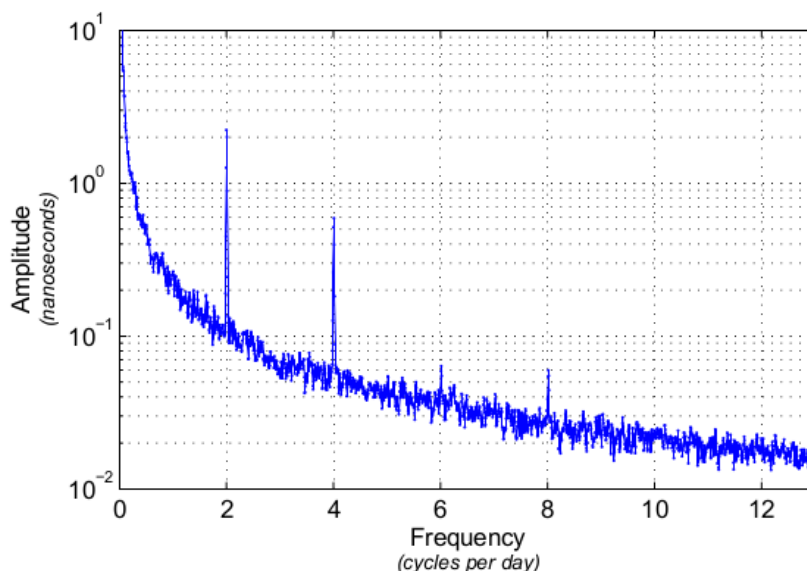

Figure 2: Amplitude spectrum for the GPS constellation clocks. Spectra were calculated individually for each satellite and averaged over the entire constellation of clocks.

3 Timescale Constraints

The geodetic estimation technique necessarily produces phase offset observations of each clock that are rank deficient in the sense that each clock's phase must be estimated with respect to the phase of some other reference clock, or timescale. The goal of a timescale algorithm is to generate a reference (paper) clock that is both stable but also independent of any single clock, or equivalently to produce better estimates of each individual clock's behavior; these are equivalent since for example estimating perfectly an individual clock is equivalent to generating a perfect reference. The rank deficiency of the phase observations represents an observability problem in estimating the individual clocks and is typically addressed by introducing additional constraints into the estimation process, typically an additional assumption(s) about how the ensemble behaves on average.

Since each type of random input–random walk phase (RWPH), random walk frequency (RWFR), and random walk drift (RWDR)–represents from an ensemble of clocks a separate ensemble of noises, three separate recursive weighted conditions are imposed to constrain the ensemble timescale solution (Stein, 1993):

$$
\begin{aligned}
\sum_{i=1}^{N} a_i(t) \cdot (x_i(t) - x_i(t|t - \delta)) &= 0 \\
\sum_{i=1}^{N} b_i(t) \cdot (y_i(t) - y_i(t|t - \delta)) &= 0 \\
\sum_{i=1}^{N} c_i(t) \cdot (w_i(t) - w_i(t|t - \delta)) &= 0
\end{aligned}
\tag{1}
$$

where the notation, $(t|t + \delta)$, denotes a prediction of the given quantity to epoch t from some previous epoch $t + \delta$. These constraints impose that the weighted sum of the differences between the clock's true states and their predictions be zero on weighted (ensemble) average. Provided the correctness of the model each clock's state differs from its prediction exactly by its random noise inputs. Thus, the optimal weights a_i, b_i, and c_i are chosen inversely to the variances of the noises contributing to each state, that is, inversely to the level of each random walk noise input. This selection of weighting has the effect of normalizing each clock's contribution to the noise of the ensemble and will typically result in a reference ensemble timescale more stable than its constituents. The additional weights also have the benefit of effectively optimizing separately the different random walk type noise contributions–RWPH, RWFR, and RWDR–perturbing each of the states x, y, and w, respectively.

An example showing the benefits of multiple clock weighting is depicted in a simulation example below (Figure 3). In the example twelve clocks were simulated from three classes of clocks, each class differentiated by differing levels of RWPH and RWFR noise. The relative levels of each simulated clock's noise are represented in the figure using the Hadamard
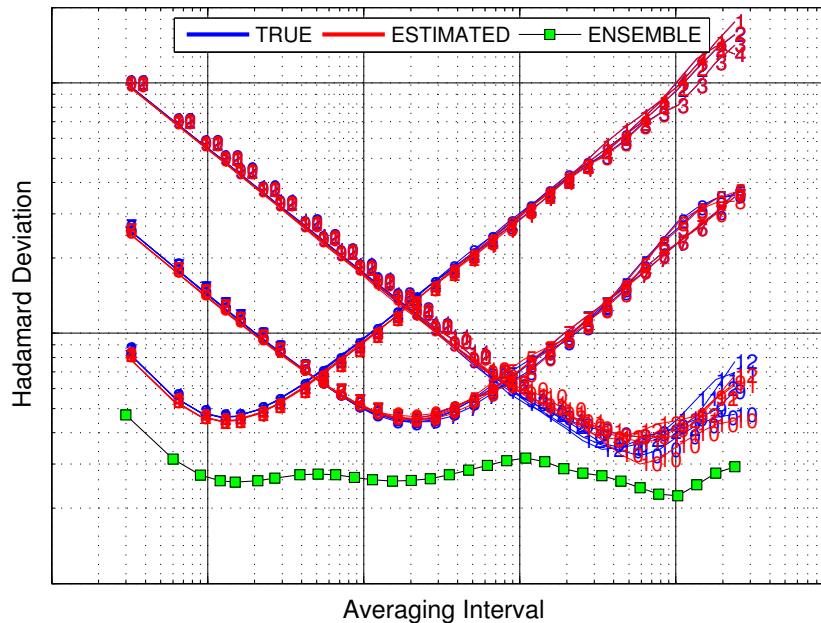
Figure 3: Timescale frequency stability results as measured by the Hadamard deviation statistic for a twelve clock simulation example based on three classes of clocks, where each class is differentiated by a relative different level of RWPH and RWFR noise.

deviation statistic where the simulated true values (blue) are plotted on a log–log scale plot of the Hadamard deviation versus averaging interval; a smaller deviation indicates lower noise at that averaging interval and the slope indicates the type of noise. Note that a slope of $-1/2$ in the plot is consistent with RWPH noise whereas a slope of $+1/2$ is consistent with RWFR. The simulated measurements were then processed in the v2.0 timescale filter with per clock weights specified inversely according to their levels of noise type. The plot also shows (green) the resulting noise of the filtered timescale. As the figure shows the ensemble timescale is more stable than any of the constituent clocks and optimally utilizes each class accordingly.

4 UTC (steering) Alignment

The steering control approach used in v2.0 to align the timescale to UTC is based on a Linear Quadratic Gaussian (LQG) drift steering control in which the amount of steering is determined via a weighted quadratic cost functional that relatively penalizes deviations of the timescale from UTC versus the relative amount of control effort (drift steering) applied. This approach is the same as that used in the legacy timescale. However, while both the legacy and v2.0 use an LQG steering control approach the UTC datum is handled

differently in the new version. In the legacy version the timescale was steered to GPS Time. The new version utilizes a weighted average of calibrated UTC(k) realizations as well as GPS Time, where the weighting is determined relative to the noise characteristics of each input, similar to the timescale clock weighting.

A method for the determination of IGS station calibration biases was determined by (Senior et al., 2004). Using information from the BIPM Circular T publication the method allows for a determination of the station clock bias offset of an IGS station clock from a collocated UTC(k) at the 1 ns level provided that the clock driving the IGS station is stable by a fixed offset relative to UTC(k) at that level. As of 2009 when the CPWG last reported on the status of the collocated stations there was sufficient timing laboratory participation in the IGS to include between five and ten IGS UTC(k) stations of sufficient quality. However, the calibration algorithm has not yet been implemented operationally in v2.0. Currently, only USN3, AMC2, and GPS Time are included as UTC steering references. These stations were included because their pseudorange data and therefore their geodetic estimates are already adjusted to compensate their UTC calibration offsets.

It is a pending CPWG item to include additional UTC(k) references.

5 Timescale Outputs

The timescale filter output includes states (from four to eight in number) and covariances for each clock relative to the ensemble timescale as well as numerous debugging and clock status information outputs. The IGS product files are re–aligned to the resulting timescale using the phase estimates from the filter in the following way. In order to avoid impacting the raw clock–clock information represented in the ACC combination clocks, the IGS clock products are not replaced directly with the phase estimates from the timescale filter. Instead, the clock measurements $z_i^r(t_k)$ that are *output* from the ACC combination and that are subsequently *input* to the timescale filter are re–aligned to a new set of measurements $z_i^e(t_k)$ relative to the ensemble timescale according to the calculation,

$$z_i^e(t_k) \triangleq z_i^r(t_k) + \text{median}_i\{z_i^r(t_k) - \hat{x}_i^e(t_k)\} \tag{2}$$

where $\hat{x}_i^e(t_k)$ are the phase estimates of each clock relative to the ensemble as determined in the timescale filter. While this retains additional measurement noise in the re–aligned products as compared to the phase estimates themselves it has the added benefit of remaining unchanged any relative clock–clock differences in the re–alignment, i.e.,

$$z_i^e(t_k) - z_j^e(t_k) = z_i^r(t_k) - z_j^r(t_k) \tag{3}$$

for any two clocks i and j. Thus, the timescale re–alignment does not impact the use of the newly align clocks in any navigation solution that uses the products.

Clock products of both the IGS Final and Rapid lines have been re–aligned to the IGS v2.0 timescales as described above, available as before in both SP3 and Clock RINEX formats. Additional timescale re–alignment information is also provided in the clock summary files as before with only one new modification that individual clock weighting now reflects multiple weights per clock. A sample of the addition made to each clock summary files by the timescale re–alignment is shown below in the Appendix A.

New timescale combination plots have also been developed to accompany the usual timescale processing outputs and may be found at `https://goby.nrl.navy.mil/IGStime/igrt.php` and `https://goby.nrl.navy.mil/IGStime/igrt.php` under the "plots_monthly" sub-directory; note that only monthly plots are currently available. Appendix B contains several samples of various plots now included.

Figure 9 shows a sample filter state/sigma output for the IGS BRUX station clock over the month of May 2012. In the plot the clock's phase estimates including harmonics (black), phase without harmonics (gray) state, frequency state (red), and drift state (blue) are plotted on separate scales along with accompanying sigmas (middle panel) and respective weights (bottom panel), all referenced to the new timescale. The legend of each plot shows any polynomials removed from the respective series for plotting as well as any phase or frequency breaks detected by the filter; for example, a frequency break was clearly detected (with lag) on 11 May in the plot shown

Figure 10 shows a sample frequency stability plot in which the Hadamard deviations of the highest weighted clocks are shown. Since each clock now has four weights in the combination all four weights are now shown in the legend. Changes to the clock combination summary files also now include the multiple weights per clock.

Figure 11 shows an example (AMC2) of another new plot recently added late in 2011 at ACC request showing the phase measurements of each clock relative to the timescale as gleaned from the measurement re–alignment described above in Equation 2. These "data vs timescale" phase–only plots more accurately reflect the timescale re–alignment actually made in the IGS product files for the reasons described above. Also, in the event that a clock has recently been added or reset within the filter its estimates may not have yet reached steady–state. Although the filter sigmas will indicate this condition these additional plots have been added for observing or monitoring clock behavior during such states.

6 Additional Features

The implementation of the v2.0 algorithm is a U–D Kalman filter that is fully automated, requiring no additional user input once the filter has been started. A new feature of the v2.0 algorithm is its ability to adaptively update the clock noise parameters corresponding to the random walks. Whenever a clock is first introduced into the timescale it's entered with

zero weights and its state and covariance are initialized using a quadratic fit procedure that reduces the otherwise large initial uncertainties of its covariance. Values for its clock model noise parameters are also initially determined automatically according to the following. The clock's RWPH level is determined relative to another stable clock using 1 day of data and using the Hadamard deviation statistic (Hutsell, 1995). Its RWFR and RWDR levels are initially set high and depend on the RWPH level determined. The adaptive filter mechanism subsequently adjusts the noise parameters adaptively utilizing the filter's innovation sequence (pre–fit residuals).

Other necessary practical features of a fully automated timescale include the ability to introduce new clocks into the timescale filter (or remove older ones) without unduly affecting the performance of the timescale. Also, the ability to respond to bad data or to a discrete change in the states of a clock as might for example occur during a station equipment change or upgrade is also necessary. These additional features have been implemented in the new v2.0 timescale.

7 Current Status of IGS Time Scales

Figure 4 summarizes the current overall phase offset status of the IGS Rapid (IGRT) and Final (IGST) timescales as compared against GPS Time and UTC from late 2010 through July 2012, utilizing information from the BIPM Circular T publication. The plot clearly shows an overall UTC alignment improvement as of the transition to version 2.0 though some remaining instabilities in the Rapid timescale are occasionally present. Although the IGS products did not transition until Spring 2011 the plot shows v2.0 data beginning at Jan 1, 2010 where the new timescale was run for this longer period before the transition.

Table 1 below shows the overall comparison of the tie to UTC before and after the transition to v2.0. The Final products now show a very tight relationship to UTC better than 3 ns over the period.

Table 1: Mean and Standard Deviation of the Rapid (IGRT) and Final (IGST) IGS timescales relative to UTC before and after the transition to v2.0.

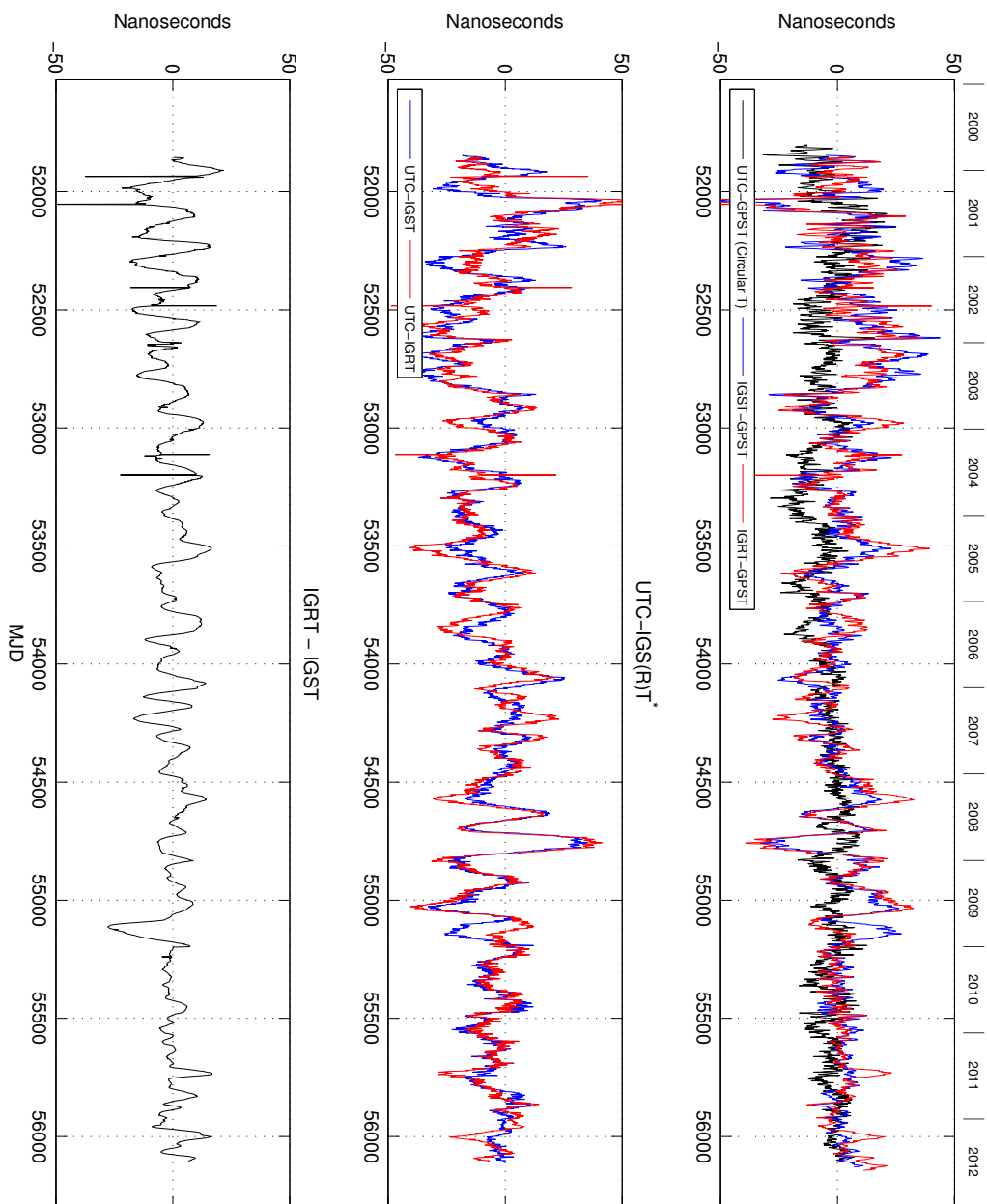|	Legacy Mean $\pm$ STD	v2.0 Mean $\pm$ STD
IGST $-$ UTC	-6.9 ± 13.1	-2.2 ± 2.7
IGRT $-$ UTC	-6.3 ± 13.7	-4.5 ± 7.9

Figure 4: IGS Timescales measured against GPS Time and UTC. Note that data on this plot from the new v2.0 timescale begins Jan 1, 2010 though the products were not transitioned until Spring 2011.
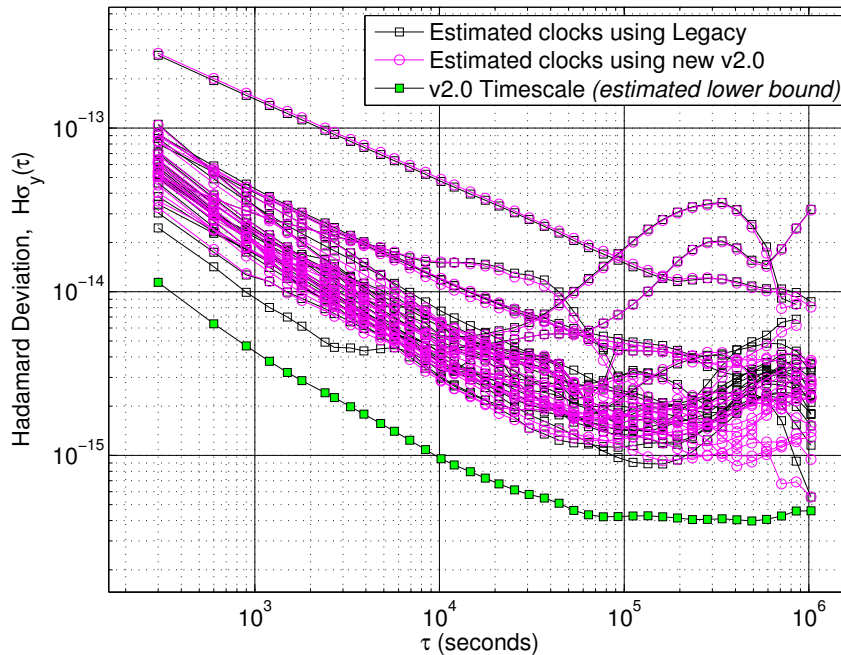
Figure 5: Instabilities (Hadamard deviation) of the most stable IGS clocks relative to the legacy (black) and new v2.0 (red) IGS timescales calculated over the first three months of 2011. Also shown is a lower–bound estimate of the resulting timescale assuming the validity of the phase estimates and the weights used during the period shown. This is a lower bound estimate of the timescale not an estimate of the timescale realized.

Figure 5 shows the frequency stability performance plot of the new v2.0 timescale compared with the legacy version as measured by the Hadamard deviation statistic. The statistics shown were calculated using IGS Final data over the first three months of 2011 and only the most stable clocks over the period are plotted. As may be gleaned by the banding of the clock estimates from each the old (black) and the new (red) versions the new version 2.0 algorithm shows improved stability over the longer term averaging intervals as desired. It's also clear that for shorter averaging intervals there's essentially no difference between the old and new versions consistent with the effectively equivalent short–term weighting constraints in both versions (inverse of RWPH levels).

As a measure of the performance consistency over time of the v2.0 timescales a histogram of the number of clocks having frequency stability as measured by the Hadamard deviation of the (internal) phase estimates better than $3 \cdot 10^{-15}$ at an averaging interval of $21,600\,\mathrm{s}$ plotted daily since 2011 is shown in Figure 6 below. As the figure shows there is generally uniform consistency over time of the performance of the products with average numbers of clocks have such stability being 16.6 ± 3 and 12.9 ± 3 for IGST and IGRT, respectively. However there are sporadic days over this period in which the number of such stabilities drops below five clocks. Because these "internal" measures of stability depend on the
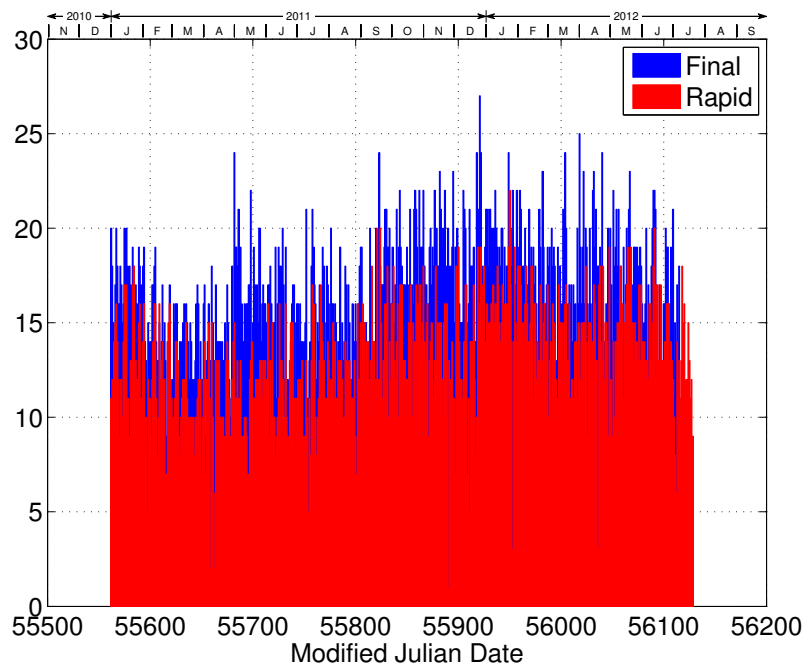
Figure 6: Histogram of the daily number of clocks in the IGS Final and Rapid timescale filters having phase estimate stabilities better than $3 \cdot 10^{-15}$ at $\tau = 21,600 \, \mathrm{s}$ as measured by the Hadamard deviation statistic.
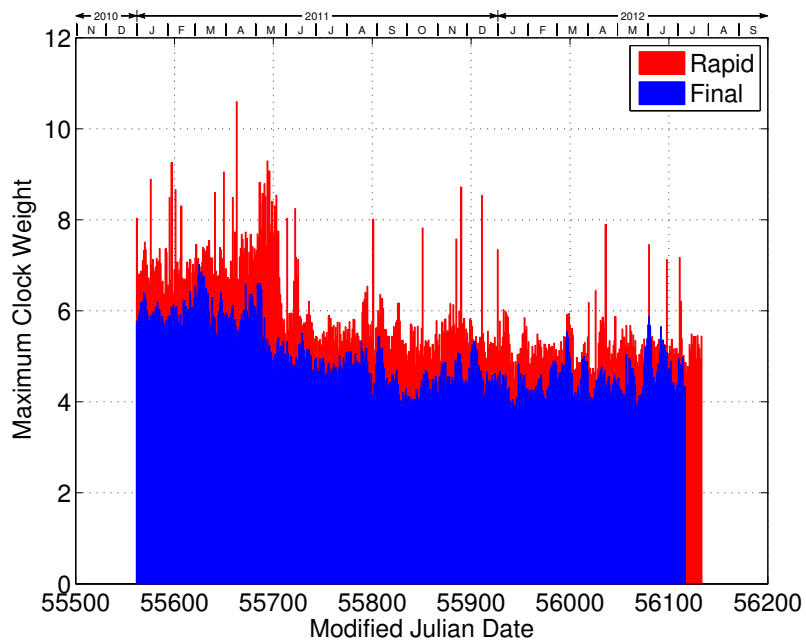
Figure 7: Maximum daily a weight (in %) per clock for the v2.0 IGS Final and Rapid timescales since 2011.

relative clock weights assigned to each clock the maximum a weight (see Equation 1) for each clock is also plotted over the same period in Figure 7.

As detailed above the addition of new fixed period harmonic states to the timescale filter was made in order better compensate the GPS constellation clock errors. Harmonics at frequencies of 2.003 and 4.006 cycles/day are estimated for each of the GPS constellation clocks in both the Rapid and Final timescales. Figure 8 below shows each of the two phase state estimates for PRN 25 versus IGST over a one week period in May 2012. The black series shows the phase state that includes the influence of the harmonics while the gray series shows the other phase state that is estimated without their influence. The magnitude of the difference between the black and gray series demonstrates both the need for estimating these harmonics as well as the effectiveness of the filter in isolating them.
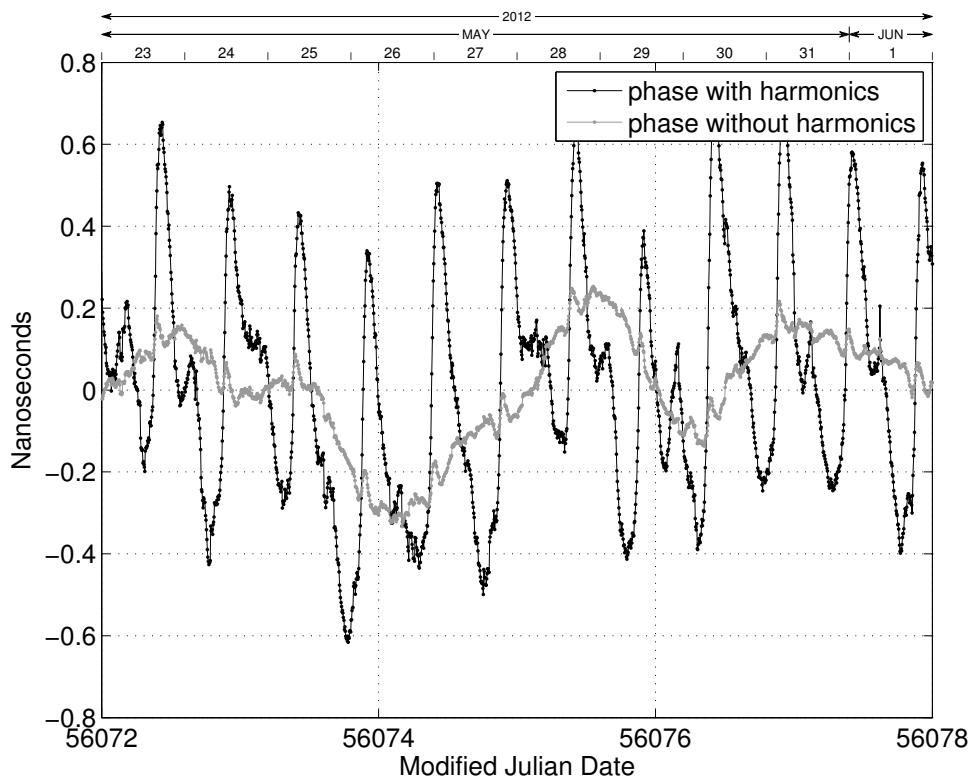
Figure 8: Timescale filter phase estimates of PRN 25 versus the IGS Final timescale IGST over the one week period 25 May through 31 May 2012. The black series shows the timescale phase state with harmonics while the gray series shows the phase minus the harmonics. An overall quadratic was removed from both series for plotting.

References

Hutsell, S. T.; 1995. Relating the hadamard variance to MCS Kalman filter clock estimation. *Proc. of the 27th Annual Precise Time and Time Interval (PTTI)* Applications and Planning Meeting, p. 293, San Diego, Calif, USA, December 1995.

Kouba J. and T. Springer; 2001. New IGS station and satellite clock combination. *GPS Solutions*, 4(4):31–36. doi: 10.1007/PL00012863.

Jones J and P. V. Tryon; 1983. Estimating time from atomic clocks. *Journal of Research of the National Bureau of Standards*, 88(1):17–24.

Montenbruck O., U. Hugentobler, R. Dach, P. Steigenberger, and A. Hauschild; 2011. Apparent clock variations of the Block IIF–1 (SVN62) GPS satellite. *GPS Solutions*, 16(3):303–313. doi: 10.1007/s10291-011-0232-x.

Senior K., P. Koppang, and J. Ray; 2003. Developing an IGS time scale. *IEEE Trans Ultrason Ferroelectr Freq Control*, 50:585–593.

Senior K., G. Petit, and J. Ray; 2004. Comparison of instrumental and empirical station timing biases for a set of Ashtech Z12T GPS receivers. *Proc. 18th European Frequency and Time Forum EFTF 2004*, Guildford, UK, 4–7, April, 2004.

Senior K., J. Ray, and R. Beard; 2008. Characterization of periodic variations in the GPS satellite clocks. *GPS Solutions*, 12(3):211–225. doi: 10.1007/s10291-008-0089-9.

Stein, S. R.; 1993. Advances in time–scale algorithms. *Proc. of the 24th Annual Precise Time and Time Interval (PTTI)* Applications and Planning Meeting, pp. 289–303, Greenbelt, Maryland, USA, December 1993.

A Sample of New Combinationa Clock Summary

Sample of New v2.0 IGS Timescale Filter Additions to the Combination Clock Summary Files:

```
RESULTS OF TIME SCALE COMBINATION:
```

	STABILITY RESULTS FROM IGS CLOCK ENSEMBLE							HADAMARD DEVIATION AT TAU =		
	NREPO	NBEPO	NFRQ BRKS	NEPO USED	MEAN WGT1(%)	MEAN WGT2(%)	MEAN WGT3(%)	MEAN WGT4(%)	300s	3600s	21600s
NISU	288	288	0	288	6.63	9.95	0.51	0.51	8.94e-15	4.08e-15	2.62e-15
BRUS	288	288	0	288	4.55	7.13	8.70	8.70	9.78e-15	7.07e-15	2.13e-15
BREW	288	288	0	288	4.54	7.10	0.67	0.67	1.04e-14	4.44e-15	1.63e-15
AMC2	288	288	0	288	3.73	4.77	5.16	5.16	1.15e-14	5.53e-15	9.16e-16
DRAO	288	287	1	288	3.73	4.77	9.97	9.97	1.13e-14	5.13e-15	4.72e-15
NLIB	288	288	0	288	3.72	4.76	7.97	7.97	1.07e-14	7.40e-15	3.61e-15
NPLD	287	286	1	287	3.71	4.73	1.24	1.24	-	-	-
USNO	288	288	0	288	3.62	4.49	0.86	0.86	1.01e-14	5.12e-15	1.87e-15
YELL	288	287	1	288	3.56	4.36	9.31	9.31	7.83e-15	4.95e-15	2.08e-15
WSRT	288	288	0	288	3.53	4.27	9.97	9.97	6.14e-15	5.73e-15	2.58e-15
STJO	288	288	0	288	3.49	4.19	5.57	5.57	7.52e-15	5.86e-15	2.55e-15
SPTO	288	288	1	288	3.24	3.59	3.97	3.97	8.20e-15	4.52e-15	2.65e-15
WES2	288	288	0	288	3.11	3.32	0.65	0.65	7.18e-15	5.83e-15	1.43e-14
NRC1	288	288	0	288	3.00	3.09	1.14	1.14	8.10e-15	8.88e-15	1.90e-15
USN3	288	288	0	288	2.95	2.97	1.53	1.53	1.71e-14	6.35e-15	1.31e-15
GPST	288	287	1	288	2.90	2.89	0.17	0.17	7.68e-15	4.47e-15	9.57e-16
CHUR	288	288	1	288	2.67	2.45	2.44	2.44	1.06e-14	7.81e-15	5.05e-15
HOB2	288	287	1	288	2.61	2.32	0.11	0.11	3.94e-14	1.70e-14	3.30e-15
KOKB	288	288	0	288	2.57	2.27	3.31	3.31	1.35e-14	1.24e-14	5.00e-15
TWTF	288	288	0	288	2.41	1.98	2.10	2.10	1.16e-14	1.39e-14	3.17e-15
NYAL	288	288	0	288	2.22	1.69	0.19	0.19	1.23e-14	2.36e-14	3.26e-14
NYA1	288	288	0	288	2.03	1.41	0.17	0.17	1.20e-14	2.33e-14	3.21e-14
BRFT	288	288	0	288	1.90	1.24	0.56	0.56	1.74e-14	1.95e-14	8.67e-15
KHAJ	288	288	0	288	1.88	1.21	0.56	0.56	1.74e-14	2.17e-14	1.74e-14
GODE	288	284	2	288	1.73	1.02	0.11	0.11	1.52e-13	4.70e-14	4.09e-14
NOT1	288	288	0	288	1.66	0.94	0.37	0.37	1.44e-14	1.35e-14	5.84e-15
USUD	288	288	0	288	1.50	0.77	0.05	0.05	8.28e-14	2.30e-14	3.75e-15
MDVJ	288	287	1	288	1.47	0.74	1.21	1.21	2.50e-14	5.82e-15	6.25e-15
MATE	288	288	1	288	1.35	0.62	1.05	1.05	1.65e-14	1.21e-14	2.59e-14
PIE1	288	287	1	288	1.33	0.60	1.92	1.92	2.97e-14	1.34e-14	3.98e-15
ALGO	288	288	1	288	1.01	0.35	0.01	0.01	2.29e-14	9.17e-15	2.80e-15
G14	288	288	0	288	0.45	0.34	0.10	0.10	4.65e-13	5.63e-14	2.34e-14
CRO1	285	285	0	285	0.91	0.28	1.50	1.50	-	-	-
G23	288	288	0	288	0.51	0.27	2.50	2.50	4.38e-13	5.35e-14	9.98e-15
G02	288	288	0	288	0.51	0.26	0.46	0.46	4.60e-13	4.27e-14	1.55e-14
G11	288	288	0	288	0.40	0.25	0.02	0.02	5.95e-13	5.81e-14	4.78e-14
IRKJ	283	280	1	283	0.81	0.23	3.43	3.43	-	-	-
G13	288	288	0	288	0.47	0.23	0.26	0.26	4.57e-13	6.08e-14	4.02e-14
G17	287	287	0	287	0.43	0.20	0.01	0.01	-	-	-
G16	288	287	0	288	0.48	0.18	2.85	2.85	5.67e-13	7.15e-14	2.90e-14
G20	288	288	0	288	0.38	0.18	4.17	4.17	5.77e-13	6.13e-14	1.57e-14
G19	288	287	0	288	0.47	0.18	0.82	0.82	5.32e-13	6.49e-14	4.43e-14
G18	288	288	0	288	0.30	0.17	0.54	0.54	7.92e-13	8.85e-14	2.52e-14
HRAO	288	288	0	288	0.67	0.15	0.10	0.10	7.60e-14	2.93e-14	4.63e-14
PTBB	288	288	0	288	0.67	0.15	0.56	0.56	1.58e-13	6.46e-14	2.60e-14
MAR6	288	288	0	288	0.62	0.13	0.00	0.00	1.59e-13	6.57e-14	3.05e-14
G07	275	275	0	275	0.42	0.13	0.00	0.00	-	-	-
G22	288	288	0	288	0.37	0.12	0.00	0.00	4.80e-13	5.51e-14	1.22e-14

G26	288	288	0	288	0.42	0.11	0.31	0.31	2.93e-13	1.30e-13	6.36e-14
G29	288	288	0	288	0.40	0.10	0.31	0.31	3.18e-13	1.17e-13	6.19e-14
PRDS	288	288	0	288	0.51	0.09	0.09	0.09	2.00e-13	7.15e-14	2.46e-14
G04	288	288	0	288	0.35	0.09	0.19	0.19	3.29e-13	1.15e-13	5.94e-14
G05	288	288	0	288	0.33	0.08	0.01	0.01	1.69e-13	5.49e-14	1.19e-13
TLSE	288	288	0	288	0.42	0.06	0.19	0.19	2.88e-13	1.12e-13	2.02e-14
BOR1	287	287	0	287	0.35	0.04	0.04	0.04	-	-	-
PIE1	288	287	1	288	1.33	0.60	1.92	1.92	2.97e-14	1.34e-14	3.98e-15
PRDS	288	288	0	288	0.51	0.09	0.09	0.09	2.00e-13	7.15e-14	2.46e-14
SPT0	288	288	1	288	3.24	3.59	3.97	3.97	8.20e-15	4.52e-15	2.65e-15
STJ0	288	288	0	288	3.49	4.19	5.57	5.57	7.52e-15	5.86e-15	2.55e-15
SYOG	288	288	0	0	0.00	0.00	0.00	0.00	6.88e-13	2.13e-13	1.71e-13
THTI	216	161	29	0	0.00	0.00	0.00	0.00	-	-	-
TIDB	288	287	1	0	0.00	0.00	0.00	0.00	7.39e-14	2.39e-14	8.39e-15
TLSE	288	288	0	288	0.42	0.06	0.19	0.19	2.88e-13	1.12e-13	2.02e-14
TWTF	288	288	0	288	2.41	1.98	2.10	2.10	1.16e-14	1.39e-14	3.17e-15
USNO	288	288	0	288	3.62	4.49	0.86	0.86	1.01e-14	5.12e-15	1.87e-15
WAB2	0	0	0	0	0.00	0.00	0.00	0.00	-	-	-
WES2	288	288	0	288	3.11	3.32	0.65	0.65	7.18e-15	5.83e-15	1.43e-14
WSRT	288	288	0	288	3.53	4.27	9.97	9.97	6.14e-15	5.73e-15	2.58e-15
YELL	288	287	1	288	3.56	4.36	9.31	9.31	7.83e-15	4.95e-15	2.08e-15
GPST	288	287	1	288	2.90	2.89	0.17	0.17	7.68e-15	4.47e-15	9.57e-16
WROC	288	243	19	0	0.00	0.00	0.00	0.00	3.35e-12	1.15e-12	1.13e-12
PTBB	288	288	0	288	0.67	0.15	0.56	0.56	1.58e-13	6.46e-14	2.60e-14
SFER	0	0	0	0	0.00	0.00	0.00	0.00	-	-	-
STR1	288	288	0	0	0.00	0.00	0.00	0.00	6.05e-13	2.16e-13	3.86e-14
SYDN	0	0	0	0	0.00	0.00	0.00	0.00	-	-	-
USN3	288	288	0	288	2.95	2.97	1.53	1.53	1.71e-14	6.35e-15	1.31e-15
USUD	288	288	0	288	1.50	0.77	0.05	0.05	8.28e-14	2.30e-14	3.75e-15
ZIMM	287	68	146	0	0.00	0.00	0.00	0.00	-	-	-
YEBE	0	0	0	0	0.00	0.00	0.00	0.00	-	-	-
WHIT	288	288	2	0	0.00	0.00	0.00	0.00	5.07e-13	5.38e-13	3.64e-13
ALBH	287	48	167	0	0.00	0.00	0.00	0.00	-	-	-
BREW	288	288	0	288	4.54	7.10	0.67	0.67	1.04e-14	4.44e-15	1.63e-15
HOB2	288	287	1	288	2.61	2.32	0.11	0.11	3.94e-14	1.70e-14	3.30e-15
MEDI	287	285	1	0	0.00	0.00	0.00	0.00	-	-	-
NISU	288	288	0	288	6.63	9.95	0.51	0.51	8.94e-15	4.08e-15	2.62e-15
NPLD	287	286	1	287	3.71	4.73	1.24	1.24	-	-	-
TNML	288	280	5	0	0.00	0.00	0.00	0.00	3.26e-13	1.28e-13	1.19e-13
TSKB	288	288	0	0	0.00	0.00	0.00	0.00	8.94e-13	2.22e-13	1.05e-13
CEDU	287	46	168	0	0.00	0.00	0.00	0.00	-	-	-
GMAS	288	275	8	0	0.00	0.00	0.00	0.00	1.00e-12	3.29e-13	1.14e-13
OUS2	287	48	170	0	0.00	0.00	0.00	0.00	-	-	-
MAD2	0	0	0	0	0.00	0.00	0.00	0.00	-	-	-
IENG	0	0	0	0	0.00	0.00	0.00	0.00	-	-	-
IRKT	0	0	0	0	0.00	0.00	0.00	0.00	-	-	-
DAEJ	287	204	48	0	0.00	0.00	0.00	0.00	-	-	-
TOW2	288	288	0	0	0.00	0.00	0.00	0.00	4.10e-13	1.16e-13	1.53e-13

STEERS APPLIED TO TIME SCALE:	9.23e-23	9.47e-23	3.04e-22

MOST STABLE CLOCKS:	WSRT	NISU	NISU

B Sample of Plots

Figure 9, page 234

> Sample plotting output of the v2.0 timescale filter states/sigmas for the IGS site BRUX. The plot shows the four base states, sigmas, and weights for the clock over a one month period.

Figure 10, page 234

> Sample combination stability plot showing the frequency stability of the highest weighted clocks in the IGS timescale for the period 1 May to 31 May, 2012.

Figure 11, page 234

> Sample "data vs timescale" plot showing the timescale input phase data for the clock at AMC2 referenced to the timescale IGST for May 2012. These phase "data" plots differ from the phase estimates as they include measurement noise but also since a clock may not be in steady–state within the filter because the clock is new or has undergone a reset.
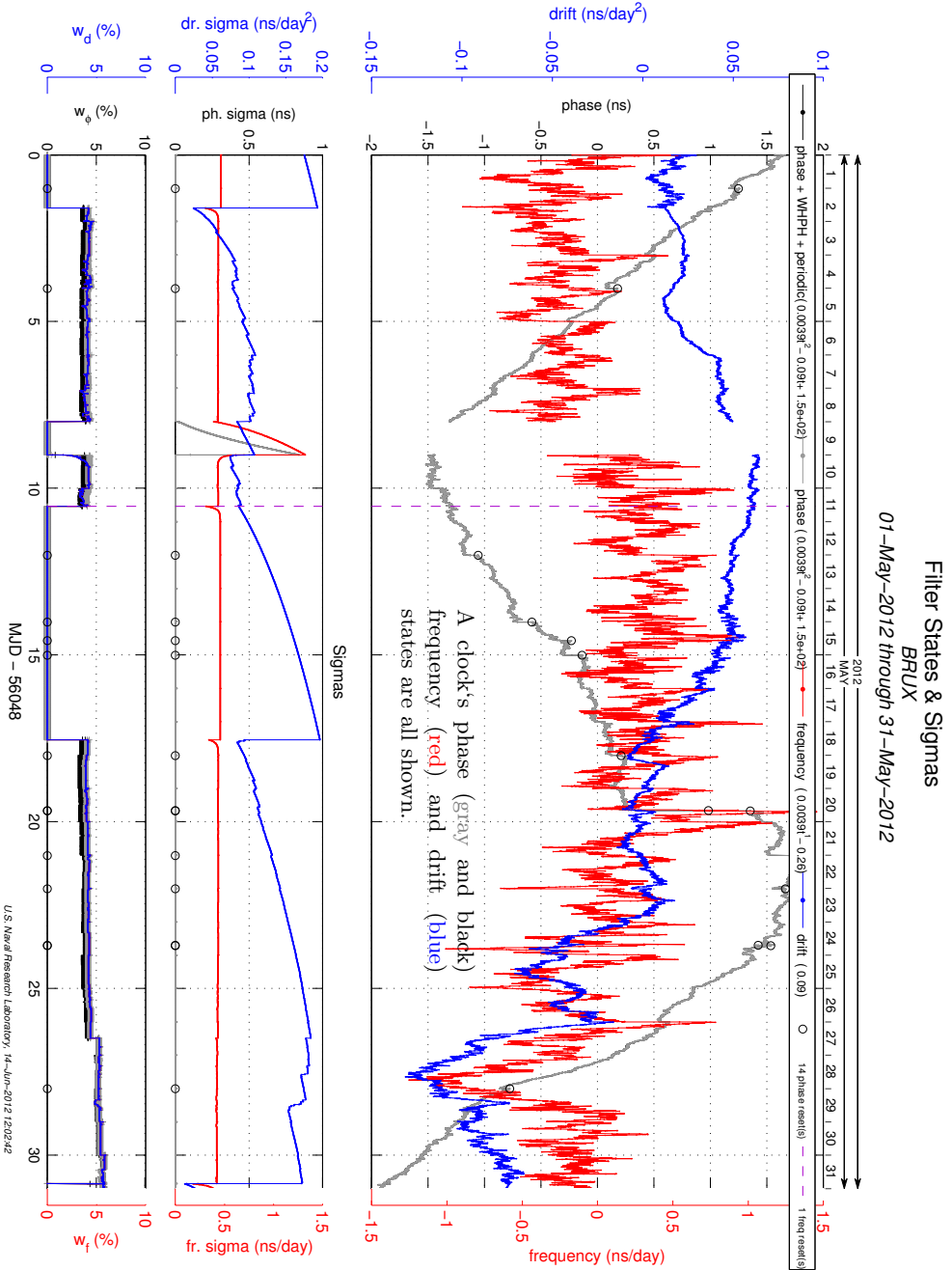
Figure 9: Sample plotting output of the v2.0 timescale filter states/sigmas for the IGS site BRUX. The plot shows the four base states, sigmas, and weights for the clock over a one month period. The black series correspond to the phase (including harmonics), the gray the phase without harmonics, the red series correspond to frequency and blue to drift. The legend also indicates any polynomials removed for plotting and/or phase or frequency breaks detected.
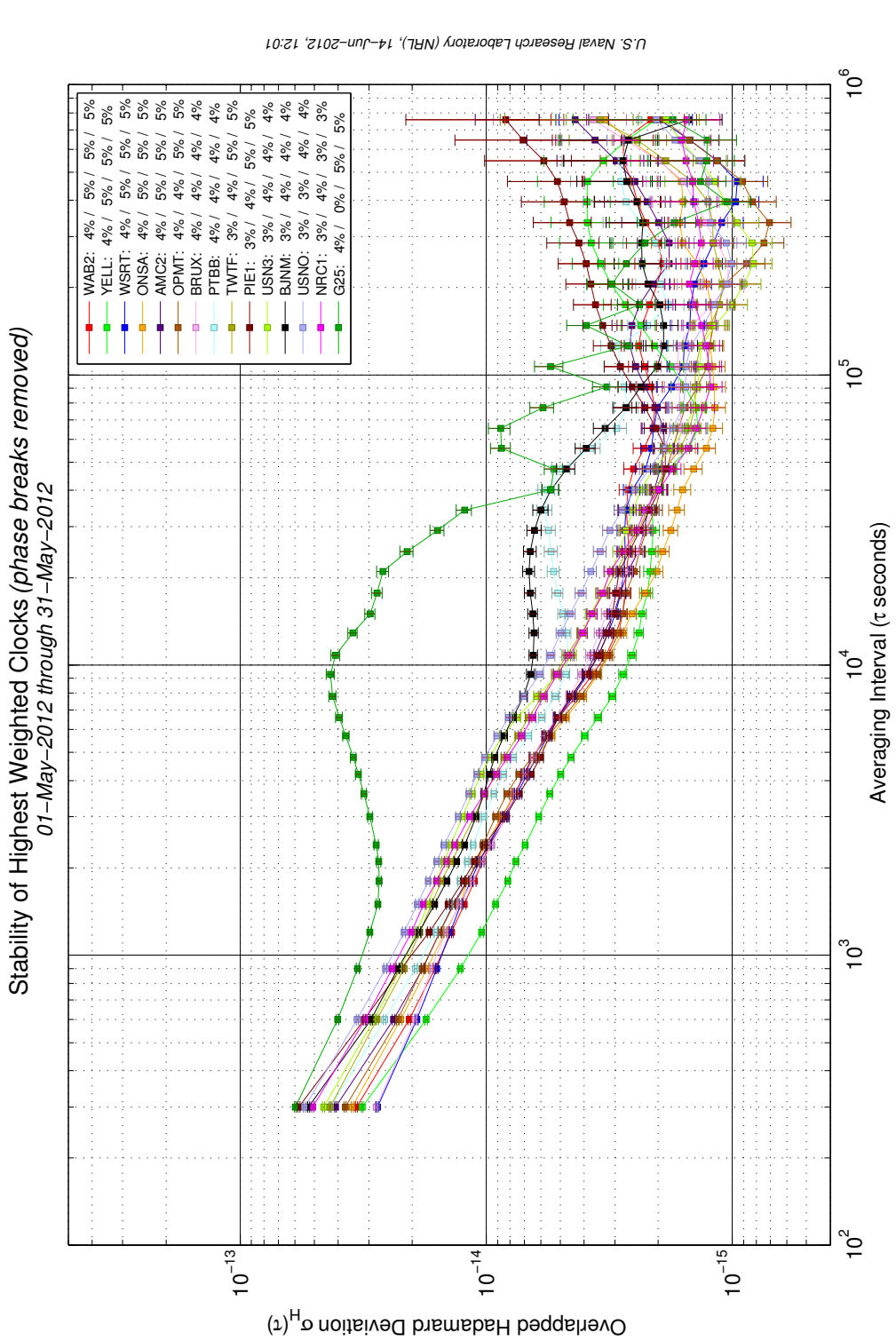
Figure 10: Sample combination stability plot showing the frequency stability of the highest weighted clocks in the IGS timescale for the period 1 May to 31 May, 2012. The a, b, c, and d weights for each clock are shown in the legend.
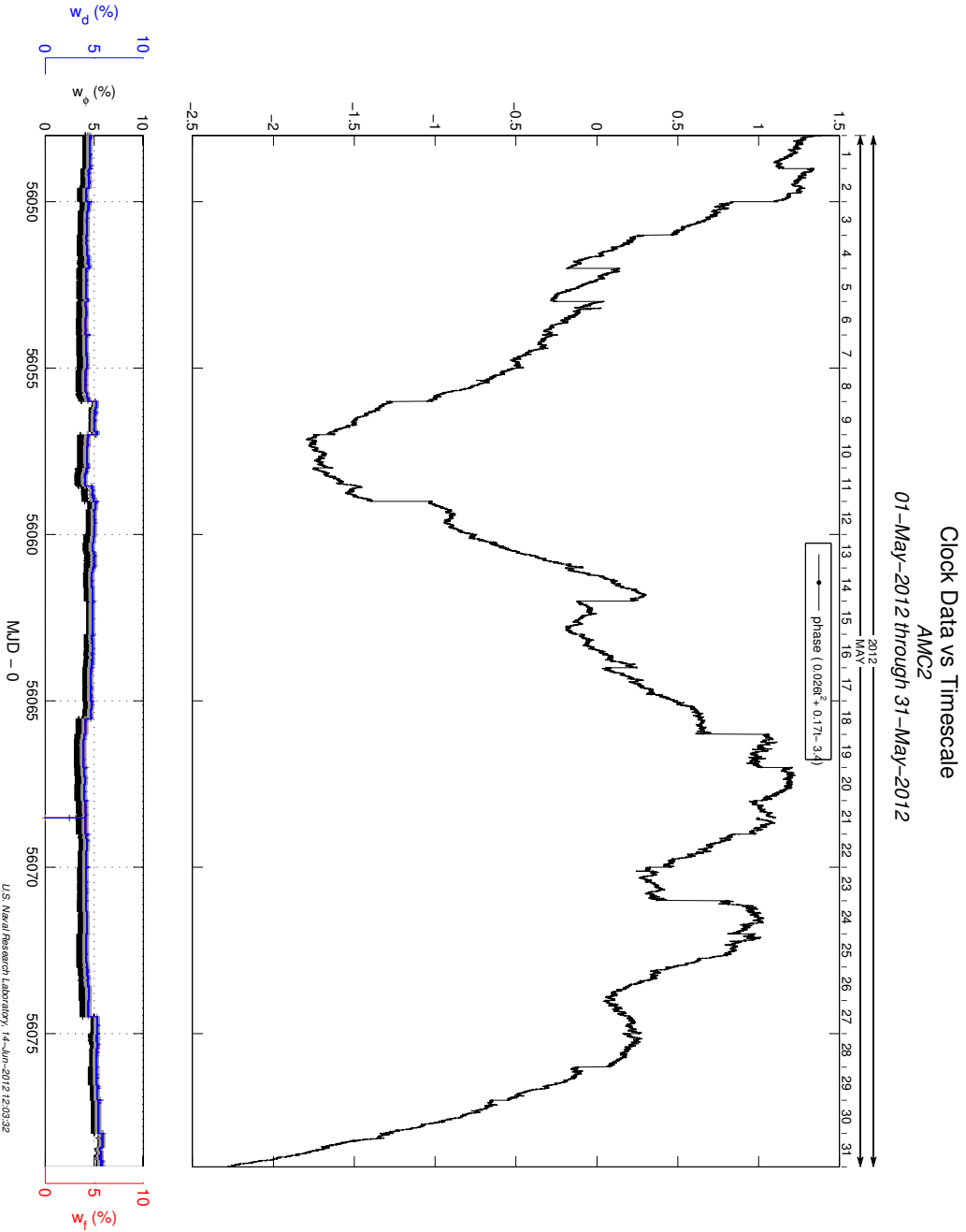
Figure 11: Sample "data vs timescale" plot showing the timescale input phase data for the clock at AMC2 referenced to the timescale IGST for May 2012. These phase "data" plots differ from the phase estimates as they include measurement noise but also since a clock may not be in steady–state within the filter because the clock is new or has undergone a reset.